Ejector Performance at High Temperatures and Pressures

Brian Quinn*
Air Force Aero Propulsion Laboratory, Wright-Patterson Air Force Base, Ohio

Attention has recently been given to the use of thrust augmenting ejectors in the wings of V/STOL aircraft. Laboratory experiments using low temperature and pressure primary air have measured high-performance levels with well-designed ejectors. The present experiments were motivated by aircraft designers' questions regarding the effects of realistic temperatures and pressures on ejector performance. The simplest geometry was used: a convergent nozzle issuing into an axisymmetric duct that entrained from and exhausted to ambient conditions. The length of the ejector was varied from 12 to 0.75 diam. Primary temperatures and pressures spanned the intervals 60 to 1000°F and 10 to 80 psig. In support of existing theory, the mass entrainment performance usually decreased with increasing primary pressure although an aeroacoustic interaction reversed the trend over small intervals. Increasing the primary temperature decreased the performance of long ejectors but had little effect on the performance of short ejectors. The results are interpreted in terms of measurements of the pressure along the wall of the mixing duct and total pressure and temperature profiles acquired at the exhaust plane of the ejector.

Nomenclature

A, A_0, A_1, A_{WET} = area, of primary flow, of entrained flow, wet by a flow
da = elemental area
C = orifice or venturi meter mass flow coefficient
C_F = skin friction coefficient
C_p = $(p(x)-P_{AMB})/(P_{BM}-P_{AMB})$ the wall pressure coefficient
c_p = specific heat at constant pressure
D = diameter of mixing duct
d = diameter of primary nozzle exit
F = thrust produced by the ejector
F_{ISEN} = thrust produced by isentropically expanding primary flow from P_{RES} to P_A
$F_2(M)$ = $M(\rho/\rho_T)(t/T)^{1/2}$ the mass flux function
$F_3(M)$ = $(p/P)(1+\gamma M^2)$, the impulse function
F = $C_F(A_{WET}/A_2)(V_{WALL}/V_2)^2\bar{q}_2A_2$ the skin friction force
L = the length of the mixing duct
M = Mach number
$\dot{m}$ = $AP(\gamma/RT)^{1/2}F_2(M)$, mass flow rate
p, P, q = static, total and dynamic pressure
$p_1, p_2, p_3, \ldots, p_{60}$ = wall pressures
$\mathfrak{R}$ = gas constant
r' = $2r/d$ dimensionless radial distance from axis of mixing duct
t, T or T_T = static and total temperature
u = velocity at a point
V = $\int_A u\, d(a/A)$ the mean flow speed where the flow area is A
x = distance downstream from the plane of injection
α = $\int (\rho/\bar{\rho})(u/V)\, d(a/A) \geq 1$, the first moment
β = $\int (\rho/\bar{\rho})(u/V)^2\, d(a/A \times \geq 1$, the skewness factor or second moment
γ = ratio of specific heats
δ = $\int (\rho/\bar{\rho})(u/V)^3\, d(a/A) \geq 1$, the third moment
ϵ = $\int (\rho/\bar{\rho})(u/V)(t/T)\, d(a/A) \geq 1$
θ = T_{RES}/T_A, the primary temperature ratio
ξ_0 = P_0/P_{RES}, the nozzle efficiency
ξ_1 = P_1/P_A, the inlet efficiency
ξ_F = $2C_F(L/D)(V_{WALL}/V_2)^2$, the friction factor
π = P_{RES}/P_A, the primary pressure ratio
ρ, ρ_T = mass density of the fluid at a point, at stagnation conditions
Φ = F/F_{ISEN}, the thrust augmentation ratio
Ψ = $\theta^{-1/2}\dot{m}_1/m_0$, the reduced mass augmentation factor

Subscripts

$0, 1, 2$ = relating to primary, entrained or mixed conditions, or their respective positions in Fig. 11
A, AMB = relating to ambient conditions
BM = relating to conditions at the throat of the bellmouth inlet
EXH = relating to conditions at the ejector's exhaust plane
RES = relating to conditions in the primary flow reservoir
$WALL$ = evaluated on a surface, or at the outer edge of its boundary layer

barred quantities = average values, as $\bar{\lambda} = \int_A \lambda d(a/A)$ is the average value of the arbitrary parameter λ.

Introduction

RECENT reports[1-7] have underscored the thrust amplification, or augmentation, of high-performance ejectors. While ejectors have seen use in a variety of applications since the last century, their present vogue derives from V/STOL aircraft concepts whose wings incorporate ejectors. The wing designs constrict the length of the device in the flow direction and, if short or compact enough, seriously degrade performance. This deterioration stems from the necessity to provide a sufficiently long flow passage for thorough mixing of the primary and entrained streams. Nevertheless, by directing efforts into the mechanics of the turbulent mixing process, many of the preceding citations succeeded in achieving high performance from relatively compact ejectors.

Received Jan. 5, 1976; revision received March 3, 1976. The author gratefully acknowledges the laboratory assistance of Howard Toms.
Index categories: VTOL Powerplant Design and Installation; Nozzle and Channel Flow.

*Research Engineer. Associate Fellow AIAA. Presently, Director of Aerospace Sciences, Air Force Office of Scientific Research, Bolling AFB, Washington, D.C.

That the prior experiments were accomplished at low pressures and ambient temperatures was their principal shortcoming. Experienced designers, skeptical of laboratory results, question the promise of high performance from ejectors driven by aircraft engine effluents. In particular, they ask what effect 1000°F primary gas temperatures, delivered at two to four atmospheres of pressure, have on ejector performance.

The results of theoretical analyses, including that reported in the Appendix, indicate that increasing the temperature of the primary fluid reduces the performance of the ejector. The cause lies in the higher velocities of the heated primary jet and, thus, in the higher ejector impact losses. Unfortunately, present analyses argue only from thermodynamics and ignore the dynamic role played by the heart of the ejector process, turbulent mixing.

Since the molecular and "eddy" viscosities of a fluid depend on its temperature, designers remain uncertain of the consequence of heating the primary stream of a compact ejector. When operated with a cold flow, the performance of the short configuration suffers from incomplete mixing between primary and entrained streams. The same configuration will experience more complete mixing when operated with the more viscous, heated primary jet. This would tend to improve performance. Present theories fail to identify which effect of heating the primary stream, higher impact losses or increased mixing, will dominate the performance of compact ejectors.

If theory is inconclusive, so too is the aggregate of prior experiments. McClintock and Hood's[8] pioneering article reported "the design of an ejector is not affected by the primary jet velocity." Other factors remaining constant, one might thus infer the independence of ejector performance and temperature, although the question received neither direct nor specific treatment by the authors. In the three volume report written by DeLeo and Wood,[9] the temperature question was confused by apparently conflicting statements: Part I data and text acclaim the independence of the secondary-to-primary mass flow ratio and the primary-to-secondary temperature ratio, but Part III analysis and text claim "an increase in ejector temperature ratio," θ in the present notation, "increases pumping performance." Rabeneck, Shumpert and Sutton[10] found very little influence of temperature ratio on ejector performance. On the basis of very limited comparisons, Armstrong[11] suggests that "thrust and temperature corrected airflow are not appreciably affected by primary-to-secondary temperature ratios."

If one factor bears responsibility for the diversity of observations in the literature it is probably the diversity of experimental devices and configurations. Encapsulated pumping devices, like that used by DeLeo and Wood, suffer from high-inlet losses which, on the other hand, are practically negligible in Armstrong's experiments. Diffusers, used selectively in some experiments, are absent or integrally included in others. Since the sensitivity of diffuser performance to the initial distribution of fluid properties is well known, it is difficult, if at all possible, to isolate the effect of temperature on the ejector from that on the diffuser. The temperature question is more appropriately addressed by experiments with the simplest, most basic configurations.

This was Reid's[12] tactic. His experiments with several simple, constant area, cylindrical ejectors clearly identified the effect of pressure ratio and length on ejector performance. Tests were conducted on ejectors with inlet area ratios less than three, lengths between three and thirty-two diameters and pressure ratios up to two. Temperatures, however, were maintained at ambient levels.

Ejector performance is most frequently characterized by the thrust Φ or mass Ψ augmentation ratios. In terms of rising vertically, Φ is more significant to V/STOL aircraft, although Ψ may become more important during transition to conventional flight. Both parameters are mutually dependent but Φ derives from a higher velocity moment and is therefore more sensitive to minor perturbations. Generally speaking, an ejector that demonstrates good Φ-performance will show equally good Ψ-performance. The reverse is usually, but not necessarily, true. The equipment available for the present experiments was only capable of measuring Ψ. The ejectors were very simple and similar to Reid's, although the inlet area ratios exceeded his by an order of magnitude. The present ratios might be found on a VTOL transport but would certainly decrease on aircraft with higher wing loadings. With the larger inlet area ratios, together with increasing the ranges of pressure to six atmospheres and temperatures to 1000°F, the present experiments were intended to complement Reid's.

Experimental Apparatus

The ejector was axisymmetric and consisted of an aluminum bellmouth machined to mate smoothly to a steel mixing duct of diameter $D=1.375$ in. The length of the mixing duct was initially 17 in. but incrementally reduced during the course of the experiments. The high-energy primary air jet was expelled through a convergent, stainless-steel nozzle of exit diameter $d=0.2656$ in., thereby producing an inlet area ratio $A_1/A_0=(D/d)^2-1=25.8$. The nozzle's exit plane was located at the throat of the bellmouth and its axis of symmetry coincided with that of the mixing duct. A special tool was constructed to assure alignment and position. The nozzle connected to a large stilling chamber through a 15-in. length of 0.5-in. i.d. stainless tubing.

Pressure taps were drilled in the wall of the mixing duct. Four of these, spaced at 90-deg intervals around the circumference of the duct, were located in the primary injection plane, i.e., the throat of the bellmouth. A difference of more than two or three hundreths of an inch of water in the pressure at these locations was never observed and the arithmetric average was called the bellmouth pressure p_{BM}. Beginning 1.1875 in. downstream from the throat, other pressure taps were drilled into the wall at 0.25 intervals. These were also spaced at 90-deg intervals around the circumference of the mixing duct, so that adjacent taps at each of the four circumference locations were one inch apart. In all, there were sixty taps that indicated wall pressures relative to ambient. These were called $p_1,p_2,\ldots,p_{60}$, beginning with the most upstream location.

Figure 1 schematically illustrates the general arrangement of the experiment. Mounting components on an optical bench with a three-axis traversing capability resolved many alignment problems. A two-axis traversing table held the thermocouple and total pressure probes that surveyed the mixing duct's exhaust plane.

Standard laboratory instruments were used to measure temperature and pressure at key locations in the apparatus and its environs. These included water or mercury filled manometers, pressure transducers and fast response thermocouples. The sixty wall pressures were sensed through a Scanivalve system whose output was displayed on the Y channel of an $X-Y$ recorder. The X channel was driven by an analog signal relating the pressure signal to its corresponding distance from the exit plane of the primary nozzle. This arrangement provided a very quick and useful description of the pressure rise along the length of the mixing duct. Explicit descriptions of the apparatus and equipment can be found in Refs. 13 and 14.

The plan of the experiments was as follows: the rate at which a measured primary mass flow entrained ambient air into the mixing duct was measured as the primary stagnation pressure was increased in regular increments up to 80 psig. This was accomplished at nominal primary stagnation temperatures of 70, 500 and 1000°F. In most instances, simultaneous measurements were made of the pressure rise along the length of the duct and the distribution of pressure and temperature across one diameter of the mixing duct's exhaust plane. After these data had been reduced and examined, a short section was cut from the end of the mixing

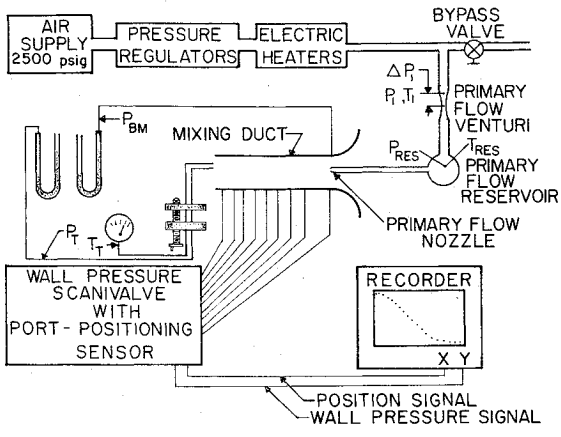

Fig. 1 Schematic diagram of experiment.

duct and the procedure repeated. This permitted the isolation of pressure, temperature and length effects on the corrected mass augmentation ratio Ψ of the ejector.

The essential parts of Ψ, the primary and secondary mass flow rates, were computed independently from equations of the form $\dot{m}_{ACTUAL} = c\dot{m}_{IDEAL}$. Ideal mass flows were computed from the compressible venturi equation using venturi pressures, temperature and geometry in the case of the primary stream, and ambient conditions expanded to the bellmouth pressure in the case of the entrained stream. Prolonged experiments,[13] in which the primary venturi and the bellmouth were tested against a venturi that had previously been calibrated by the National Bureau of Standards, provided accurate values of the flow correction coefficients. The accuracy of the corrected mass flow ratios reported in the following is estimated at ± 1 to 2%.

Results and Discussion

Performance data appear in Figs. 2 and 3, where the corrected mass augmentation ratio Ψ has been plotted against the primary pressure ratio π. The primary temperature ratios θ and lengths, L/D of the ejectors' mixing duct serve as curve parameters. The monotonically decreasing trend of $\Psi(\pi)$ exhibited by the longer ejectors supports the analytical results drawn over the $L/D = 12.36$ data for $\theta = 1.0$ and $\theta = 2.7$. The calculations employed measured[13] relationships between state variables and the nozzle ξ_0 and inlet ξ_I efficiencies, but the effect of length entered indirectly through its influence on the friction ξ_F and skewness β factors. $\xi_F = 0.1$ follows, approximately, from assuming $V_{WALL} = V_2$, the turbulent skin friction coefficient $C_F = 0.004$ and taking $L/D = 12.4$. Analysis of the $\pi = 1.7$ profiles exhausting from the $L/D = 12.36$ ejector suggested $\beta = 1.014$. Assuming the constancy of ξ_F and β across the range $1 < \pi < 7$ is, of course, naive. On the other hand, equations printed in the Appendix suggest that friction and profile characteristics appear in combination, as $(\xi_F + \beta)$. There is an exception in Eq. (A5), where the first velocity moment α appears alone, but with little influence since $(\alpha - 1) \approx .25$ $(\beta - 1) \approx 0$ for longer ejectors. Integration of the velocity profiles discussed in the following shows that the sum of ξ_F and β, and their combined effect on Ψ, did, in fact, remain nearly constant over the pressure range in question. Factors that increase β by concentrating energy along the axis of the duct tend also to reduce ξ_F by decreasing V_{WALL} relative to V_2.

So long as β and ξ_F remain independent of thermodynamics, theory stresses that higher temperatures degrade performance at all pressures. In Fig. 2, this is clearly the trend of the $L/D = 12.36$ data, where the long duct assures nearly complete mixing at all pressures. Very subtle changes that reflect the real thermodynamic dependence of β and ξ_F occur as the ejectors become shorter. The first indication appears in the $L/D = 8.73$ and 6.55 data obtained at the higher pressures.

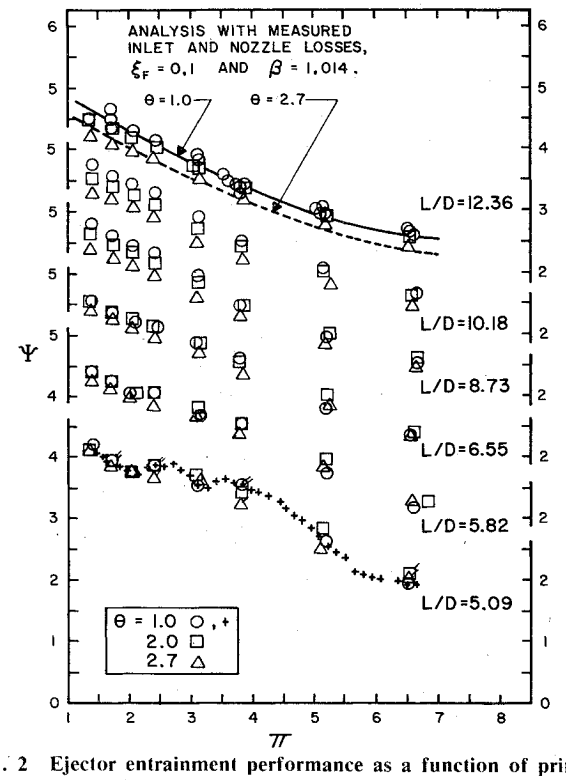

Fig. 2 Ejector entrainment performance as a function of primary pressure ratio with primary temperature ratio and the length of the ejector as curve parameters.

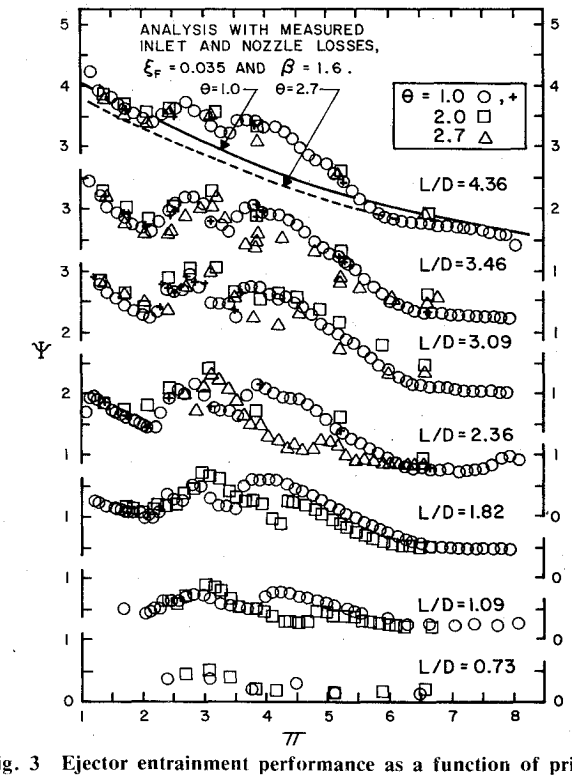

Fig. 3 Ejector entrainment performance as a function of primary pressure ratio with primary temperature ratio and the length of the ejector as curve parameters.

Notice, especially at $\pi = 5.2$ and 6.6, that the $\theta = 1$ and $\theta = 2$ data are practically coincident. At these pressures notice also that performance at $\theta = 2$ exceeds that at $\theta = 1$ for the next shorter ejector, $L/D = 5.82$. As L/D decreases from 12.36 to 5.82, the general trend is a reduction in the sensitivity of performance to θ and, in some cases, a positive influence of θ.

This tendency continues with further reductions in length, although obscured to some extent by another phenomenon.

The initial set of data obtained with the $L/D=5.09$ ejector appeared to contain more scatter than had been seen in earlier tests. The suspected points were repeated but fell perfectly on the original values, as shown by the single and double tick marks in Fig. 2. Suspicions of a departure from the monotomic trend of $\Psi(\pi)$ were confirmed by data collected at 2-psi increments throughout the interval $1.4 \leq \pi \leq 6.6$. The more refined tests clearly identified two relative maxima in Ψ, and $\pi=2.8$ and 3.8, approximately, which continued throughout the remainder of the experiments. As the length of the ejector dropped below four diameters, it became apparent, Fig. 3, that higher temperatures slightly increased the pressure levels at which the maxima were observed. Data obtained at $\theta=2.0$ and 2.7 appeared to maximize at $\pi=3.1$ and a second pressure ratio around 4.5 to 5.0. The second relative maximum was not more precisely determined because prolonged testing at elevated temperatures provoked failures in the electrical heaters which, at that time, were irreparable. The reader will notice that the three last tests, $L/D=1.82$, 1.09 and 0.73 could not be run at $\theta=2.7$.

The theoretical curves drawn over the $L/D=4.36$ data in Fig. 3 direct attention to the substantial increases in performance found in the two relative maxima. Friction and skewness factors of $\xi_F=0.035$ and $\beta=1.6$ give reasonable estimates of the performance of an $L/D=4.36$ ejector, except over pressure intervals around $\pi=2.8$ and 3.8. To achieve analytical levels of Ψ that match the measured levels at these pressure ratios requires skewness factors of $\beta=1.02$. In other words, around $\pi=2.8$ and 3.8 an extraordinary agent has nearly completely mixed the primary and entrained streams in a very short distance, 4.36 duct diameters.

Shortly after noticing the relative maxima in Ψ, abrupt changes in the noise radiating from the ejector were observed to occur repeatably at certain pressures. It was later learned that Reid[12] had observed a similar phenomenon. Quick calculations indicated that screech tones generated by the underexpanded primary jet might tune to transverse waves standing in the mixing duct around $\pi=2.8$ and 3.8 at ambient primary temperatures. Rosfjord and Tom's[15] experiments argue in favor of an influence of temperature on the tuning pressure. It would appear that the relative performance maxima were the consequence of an aeroacoustic interaction that promoted very rapid mixing. This notion was discussed briefly in Ref. 16 and will be developed more completely in the future.

Friction and mixing combine to increase the pressure of the fluid as it flows through the ejector. The contribution of friction is relatively small however, and the pressure distribution along the wall emphasizes the history of the mixing process. The data presented in Figs. 4 and 5 describe the increase in pressure or, equivalently, the reduction in $C_p=[p(x)-P_A]/[p_{BM}-P_A]$, along the wall of the $L/D=8.73$ ejector under different primary stagnation conditions. Similar trends were observed with all ejectors whose lengths exceeded their diameters by a factor of six or more. The broken line drawn for $0 \leq x/D < 1$ represents data obtained by probing through the bellmouth into the mixing duct along a path $r=D/4$ with $\theta=1$ and $P_{RES}=5$ and 50 psig. The agreement between the wall and the probe data over their common interval suggests the absence of normal pressure gradients.

The flattening of the wall pressure distributions well within the limits of the mixing duct suggests that mixing is nearly complete, that the initial, almost discontinuous profiles have evolved into almost uniform, equilibrium profiles. Moreover, the rate of change in C_p reflects the rate of mixing, and the data in Fig. 4 identify three distinct mixing rates. The fastest mixing occurs during the aeroacoustic interaction at $\pi=3.8$. An intermediate rate of mixing developed at $\pi=1.7$, 2.4 and 3.1, whereas data obtained at the highest reservoir pressures, $\pi=5.2$ and 6.6, clearly indicated retarded mixing. Similar

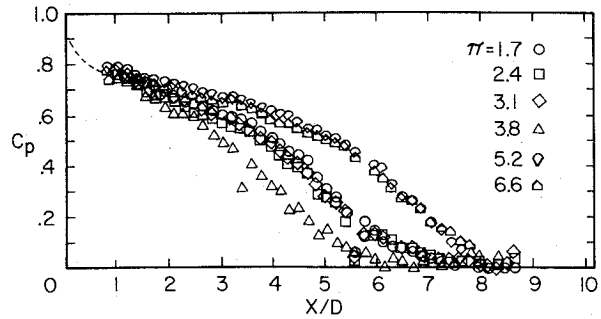

Fig. 4 Pressure distribution along the wall of the mixing duct, $L/D=8.73$, $\theta=1.0$.

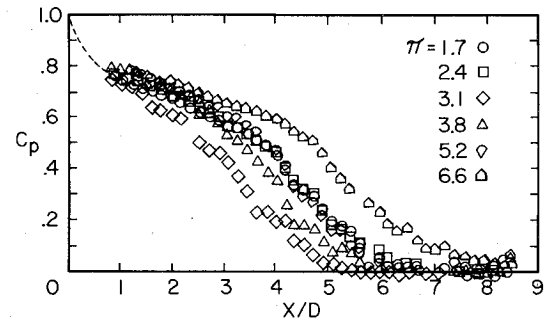

Fig. 5 Pressure distribution along the wll of the mixing duct, $L/D=8.73$, $\theta=2.7$.

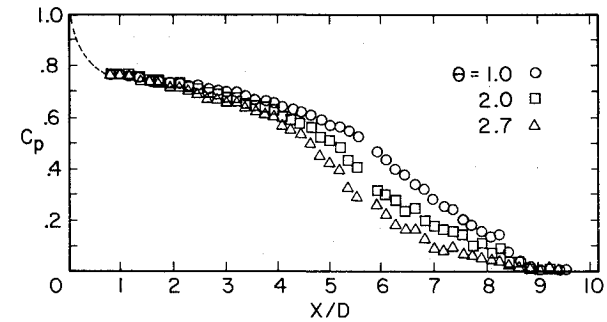

Fig. 6 Effect of primary temperature ratio on the pressure distribution through the mixing duct, $L/D=10.18$, $\pi=6.6$.

developments can be seen in Fig. 5 where the most rapid mixing also occurs during the acoustic interaction, $\pi=3.1$ when $\theta=2.7$.

A dependence of mixing rate on pressure ratio was expected, but not the identification of discrete mixing modes. The usually accepted turbulent eddy viscosity models relate mixing rates to differences in the kinematic and thermodynamic properties of two streams. While the initial differences between the primary and secondary streams certainly varied in the present experiments, they varied monotonically, not discretely, with pressure ratio. If one were to excuse the aeroacoustic data as the product of an altogether different energy transfer mechanism, the remaining data would continue to describe two discrete mixing modes. This departure from what had been expected remains unexplained.

In support of the performance data and most viscosity models, the wall pressure data show that mixing is accelerated by heating the primary stream. This can be seen by contrasting Figs. 4 and 5 or by examining Fig. 6. In making these comparisons, one must focus attention on data that derive from the same model of mixing. To do otherwise would confuse temperature effects with those attributable to other factors.

The data presented in Fig. 7 are typical of the velocity and temperature profiles measured at the mixing duct's exhaust

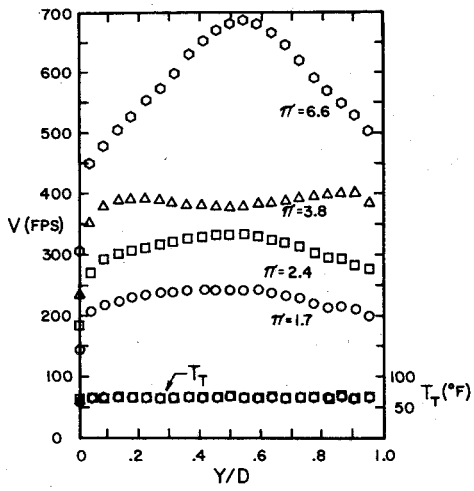

Fig. 7 Velocity and temperature profiles measured across the exhaust plane of the mixing duct, $L/D = 10.18$, $\theta = 1.0$.

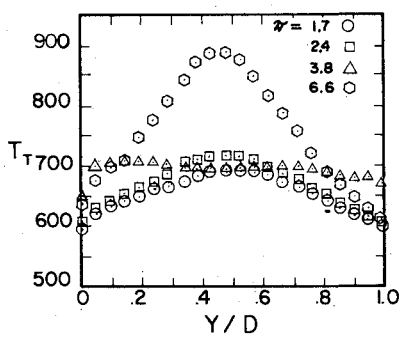

Fig. 8 Total temperature profiles measured across the exhaust plane of the mixing duct, $L/D = 5.09$, $\theta = 2.5$.

plane. Asymmetry persisted despite efforts to eliminate it by adjusting the alignment of the nozzle and duct. Armstrong[11] also discussed the attraction of axisymmetric ejector flows for one side or another of the mixing duct. The tendency, together with a random flapping from side to side, seems to have been much more pronounced in his experiments than in these. The effect on mass entrainment performance of purposely misaligning the flow was found to be slight. Differences in the four bellmouth pressures quickly registered lateral displacements of the nozzle from the centerline of the duct but remained insensitive to angular excursions less than around ten degrees, far more than indicated by the data of Fig. 7.

It is interesting to discuss Fig. 7 in light of Fig. 4. As mentioned earlier, the most rapid mixing occurs during the acoustic interaction, at $\pi = 3.8$. In contrast to tests at other pressure ratios, the velocity profiles at this condition attain their maximum values not on the centerline of the duct, but nearer to its walls. The triangles in Fig. 7 show the double peak trend which becomes more pronounced as the length of the ejector decreases. The similarity between the data obtained at $\pi = 1.7$ with those at $\pi = 2.4$ is apparent: both profiles are relatively flat and roll off near the wall. These measurements derive from the intermediate rate of mixing described by the central trace in Fig. 4. The upper trace, indicative of retarded mixing, corresponds to the very steep profile, $\pi = 6.6$, in Fig. 7. When the primary jet was heated, Fig. 8, similar trends developed in the temperature profiles but to a far less extent, consistent with faster diffusion of scalar quantities. Consistency in the stories told by Figs. 4, 7 and 8 supports the existence of several modes of mixing, an apparently fruitful research area.

Summary and Conclusions

Figures 9 and 10 are cross plots of Figs. 2 and 3 and summarize the interplay between primary state variables and length. Curves have been drawn through the cold data, $\theta = 1.0$, for clarity. An ejector of area ratio 25.8 requires a mixing duct at least half as long as its diameter in order to function. Increasing length up to around six diameters rapidly

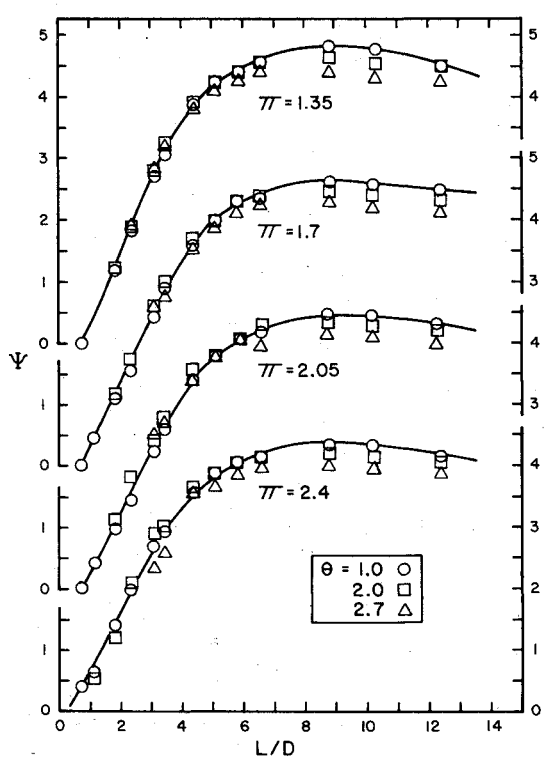

Fig. 9 The dependence of mass augmentation performance on the length of the mixing duct for parametric levels of the primary temperature and pressure ratios.

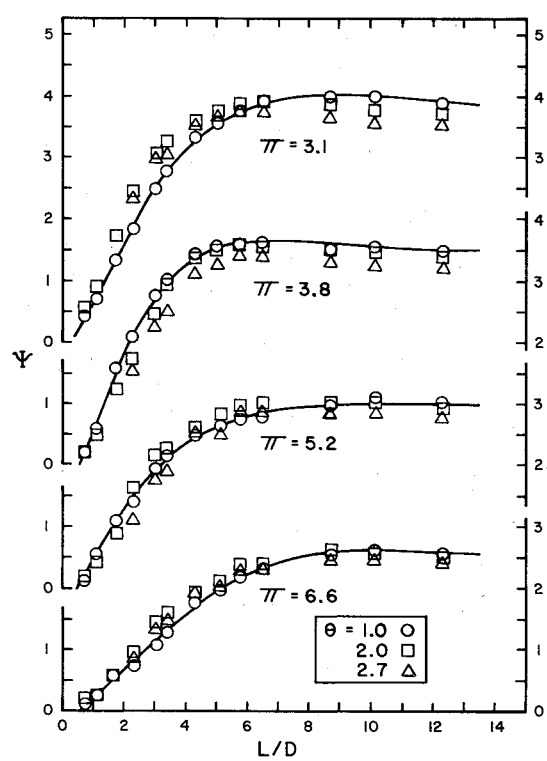

Fig. 10 The dependence of mass augmentation performance on the length of the mixing duct for parametric levels of the primary temperature and pressure ratios.

improves performance, almost linearly, by providing more time for the primary stream to transfer its energy to the entrained stream. Heating the primary fluid has a slightly favorable, if any, effect on performance in this regime because the larger viscosities reduce the skewness of the flow in the same length of mixing duct. The observation has special significance to those accustomed to thinking of the deleterious effect of temperature on the performance of fully mixed ejector flows. Performance maximizes around $L/D=9$, consistent with Reid's [12] observations. However, the peaks of the curves are rather flat and performance at $L/D=6$ differs little from the maximum. Since hot and cold flows are all well-mixed in an ejector of this length, increasing primary flow temperatures decreases performance in accordance with fully mixed ejector analyses. Increasing lengths beyond nine diameters decreases ejector performance through the integrated effect of wall friction. The principal benefit of increasing the rate of mixing, by acoustic coupling or other means, can be seen in the data obtained at $\pi=3.8$, Fig. 10. With the acoustically enhanced mixing, performance maximizes with approximately half the length usually required.

Appendix

Ejector Theory

At station 1 in Fig. 11, primary fluid flows through an area A_0 and the entrained fluid flows through an area A_1. The streams mix in a duct of constant area A_2 so $A_0+A_1=A_2$ if the primary nozzle has a vanishing wall thickness.

Assume the following. 1) Pressure is constant, but not necessarily equal, in A_0, A_1 and A_2. p_1 and p_0 equate so long as the primary nozzle remains unchoked. 2) $T_1=T_A$ and $T_0=T_{RES}$. 3) $\gamma=1.4$ and constant (this assumption has been relaxed in many computations although no significant difference was observed across the interval $1\le\theta\le3$). 4) Adiabatic flow in the mixing duct.

With these assumptions and definitions, equations can be written that express balances of mass, momentum and energy between stations 1 and 2. Thus, the following:

1) Continuity equation

$$\dot{m}_0+\dot{m}_1=\dot{m}_2$$

$$(\rho AV)_0+(\rho AV)_1=\int_{A_2}\rho u\,da=\alpha(\rho AV)_2$$

or

$$A_0\,P_0\,F_2(M_0)\,(\gamma/\Re T_0)^{1/2}+A_1\,P_1\,F_2(M_1)\,(\gamma/\Re T_1)^{1/2}$$
$$=\alpha A_2\bar{P}_2\,F_2(\bar{M}_2)\,(\gamma/\Re\bar{T}_2)^{1/2} \tag{A1}$$

2) Impulse equation

$$(p+\rho V^2)_0A_0+(p+\rho V^2)_1A_1=\mathfrak{F}+p_2A_2+\int_{A_2}\rho u^2da$$
$$=\mathfrak{F}+p_2A_2+\beta\bar{\rho}_2V_2^2A_2 \tag{A2}$$

where $\mathfrak{F}$ represents the sum of flow-directed body forces acting on the fluid as it passes through the duct. In the present example, these are friction forces that are assumed to have the form

$$\mathfrak{F}=C_F(A_{WET}/A_2)\,(V_{WALL}/V_2)^2\,\tfrac{1}{2}\bar{\rho}V_2^2A_2=\xi_F\gamma p_2M_2^2A_2$$

where the parameter

$$\xi_F=2C_F(L/D)\,(V_{WALL}/V_2)^2$$

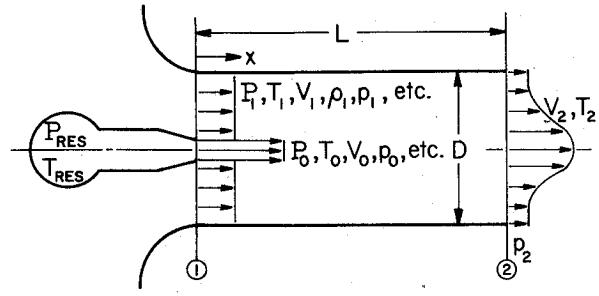

Fig. 11 Nomenclature and scheme of analytic model.

Usually, $V_{WALL}/V_2<1$, although the inequality could reverse for the extraordinary profiles produced by the aeroacoustic interaction discussed in the text.

Using the earlier definitions, Eq. (A2) becomes

$$P_0A_0F_3(M_0)+P_1A_1F_3(M_1)=p_2A_2]1+\gamma(\xi_F+\beta)M_2^2] \tag{A3}$$

3) Energy equation

$$(\dot{m}T)_0+(\dot{m}T)_1=\int_{A_2}\rho uTda=\int_{A_2}\rho u(t+(u^2/2c_p))\,da$$

or

$$T_2/T_0=\mathcal{K}\alpha/\epsilon[\,(\dot{m}_0+\dot{m}_1T_1/T_0)/(\dot{m}_0+\dot{m}_1)\,] \tag{A4}$$

where $\mathcal{K}=1+(\delta/\epsilon-1)(1-\bar{t}_2/T_2)$, a weak function of M_2. The largest value attainable by $\mathcal{K}$ occurs when the duct chokes, i.e., $M_2=1$. Moreover, as shown below, both δ and ϵ usually exceed unity by small factors which roughly confine their ratio to the interval $1\le\delta/\epsilon<1.5$. This observation assigns $\mathcal{K}$ to the interval $1\le\mathcal{K}\le1.08$ and experience indicates that setting $\mathcal{K}=1$ produces no meaningful error in performance calculations.

Dividing the continuity Eq. (A1) into the impulse Eq. (A3) and algebraically gathering terms eventually yields a biquadratic equation for the mixed flow Mach number

$$M_2^4[\alpha^2(\gamma-1)F_4^2/2-\gamma^2(\xi_F+\beta)^2]+M_2^2[\alpha^2F_4^2$$
$$-2\gamma(\xi_F+\beta)]-1=0 \tag{A5}$$

where

$$F=\frac{\pi F_3(M_0)+F_3(M_1)\,(A_1/A_0)\,(\xi_1/\xi_0)}{[\pi F_2(M_0)+F_2(M_1)\theta^{1/2}\,(A_1/A_0)\,(\xi_1/\xi_0)\,](T_2/T_0)^{1/2}}$$

With A_1/A_0, π and θ given, and with ξ_1 and ξ_0 prescribed by experiment or parametrically assigned, F_4 becomes uniquely determined by the entrained flow Mach number M_1. The corresponding value of M_2 then follows from Eq. (A5) if values have been assigned to ξ_F, α and β. In this regard, turbulent skin friction coefficients around 0.004 provide reasonable values of ξ_F. The remaining two parameters, α and β, are properties of the velocity and temperature profiles at $x=L$. Their values are, strictly speaking, independent and cannot be specified a priori, except by speculation and experience. In practice, this complication all but dissolves because an assortment of density and velocity distributions indicates that α,β, and δ are almost linearly related. Specifying one therefore specifies the other two, a situation reminiscent of the relationship between the shape factors common to boundary-layer calculations. If, for example, one assumes that u, ρ and t can be described by a distribution of the form $\lambda=1+Yf(r',X)$, the integrals that define α,β,δ and ϵ $(=\beta$

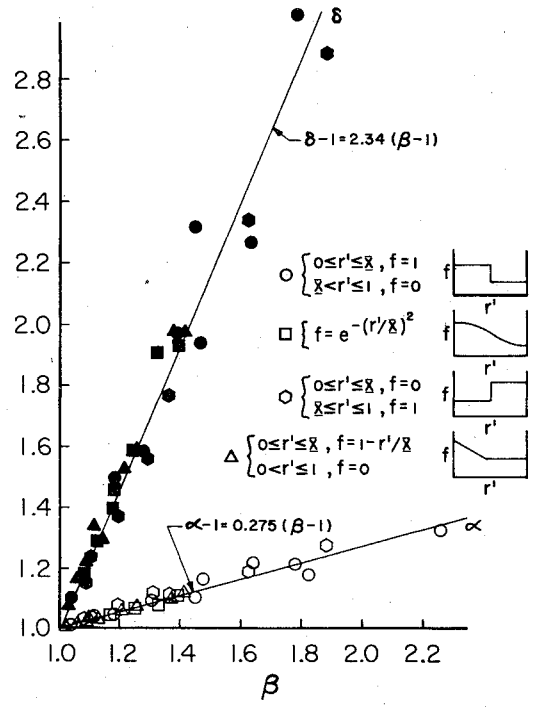

Fig. 12 Corresponding values of α and β (open symbols) and δ and β (filled symbols) computed from forty-eight different profiles.

for the distributions considered) are readily evaluated. Figure 12 was prepared by assigning twelve combinations of X and Y to each of the four profiles sketched thereon, computing the moments and plotting the related pairs (β,α) and (β,δ). In subsequent ejector performance calculations, β was arbitrarily chosen as the characterization of flow skewness, with α and δ computed by the linear functions drawn in Fig. 12.

In aircraft applications, the ejector exhausts to a pressure p_{EXH} which could differ somewhat from P_A if aerodynamic circulation were present. Assuming the existence of a diffuser or other device whose pressure rise is characterized by the coefficient $C_p=(p_{EXH}-p_2)/q_2$, the momentum Eq. (A3) can be restated as a compatibility equation:

$$(p_{EXH}/P_A)-C_p(q_2/P_A)=[\xi_0F_3(M_0)(A_0/A_2)\pi + \xi_1F_3(M_1)(A_1/A_2)][1+\gamma(\xi_F+\beta)M_2^2]^{-1} \quad \text{(A6)}$$

This relationship will be satisfied only if the proper value of M_1 has been used in Eq. (A5) to compute M_2. In practice, a computer code treats A_0,A_1, the ξ's, α, β, etc. as parameters and iterates on M_1 until Eq. (A6) has been satisfied to a specified degree of accuracy. The left-hand side of the preceding equation was, of course, unity in calculation used to support the present work.

With M_1 so determined, the performance of the ejector follows directly. Recalling,

$$\dot{m}_0=A_0P_0F_2(M_0)(\gamma/\Re T_0)^{1/2}$$

$$\dot{m}_1=A_1P_1F_2(M_1)(\gamma/\Re T_A)^{1/2}$$

then

$$\Psi=\theta^{-1/2}\dot{m}_1/\dot{m}_0=(A_1/A_0)(\xi_1/\xi_0)[F_2(M_1)/F_2(M_0)]\pi^{-1} \quad \text{(A7)}$$

The thrust F_{ISEN} produced by isentropically expanding the primary mass flux to ambient pressure is $F_{ISEN}=\dot{m}_0V_{ISEN}$, and the thrust produced by the ejector is

$$F=\int_{A_{EXHAUST}}[(p-P_A)+\rho u^2]\,da$$

For the constant area geometry used in the present experiments wherein the exhaust pressure was ambient, the ejector thrust may be written

$$F=\beta\,\bar{\rho}_2V_2^2A_2$$

The thrust augmentation ratio becomes

$$\Phi=F/F_{ISEN}=(\beta/\alpha)(\dot{m}_2/\dot{m}_0)(V_2/V_{ISEN}) \quad \text{(A8)}$$

where

$$V_2=M_2(\gamma\Re T_2)^{1/2}[1+M_2^2(\gamma-1)/2]^{-1}$$

$$V_{ISEN}=M_{ISEN}(\gamma\Re T_0)^{1/2}[1+M_{ISEN}^2(\gamma-1)/2]^{-1}$$

$$M_{ISEN}=2/(\gamma-1)[\pi^{-(\gamma-1)/\gamma}-1]^{1/2}$$

Other figures of merit such as energy transfer efficiency and pumping pressure ratio are also computable.

References

[1] Fancher, R. B., "Low Area Ratio Thrust Augmenting Ejectors," *Journal of Aircraft*, Vol. 9, March 1972, pp. 243-248.

[2] Quinn, B., "Compact Ejector Thrust Augmentation," *Journal of Aircraft*, Vol. 10, Aug. 1973, pp. 481-486.

[3] Throndson, L. W., "Compound Ejector Thrust Augmentation Development," Paper No. ASME 73-G7-67, Washington, D.C., 1967.

[4] Bevilaqua, P. M., "An Analytic Description of Hypermixing and Tests of an Improved Nozzle," *Journal of Aircraft*, Vol. 13, Jan. 1976, pp. 43-49.

[5] Streiff, H. G. and Henderson, C., "Ejector Thrust Augmentation for STOL Aircraft Applications," AIAA Paper 74-1192, San Diego, Calif., Oct. 1974.

[6] Schweiger, M. and Tankursley, J., "XFV-12A Ejector Wing Tests," AIAA Paper 74-1193, San Diego, Calif., Oct. 1974.

[7] Campbell, D. R. and Quinn, B., "Test Results of a VTOL Propulsion Concept Utilizing a Turbofan Powered Augmentor," *Journal of Aircraft*, Vol. 11, Aug. 1974, pp. 467-471.

[8] McClintock, F. A. and Hood, J. H., "Aircraft Ejector Performance," *Journal of the Aeronautical Sciences*, Vol. 13, Nov. 1946, pp. 559-568.

[9] DeLeo, R. V. and Wood, R. D., "An Experimental Investigation of the Use of Hot Gas Ejectors for Boundary Layer Removal," WADC Technical Rept. 52-128 (AD 155 609), Part I, Apr. 1952, Part II, Dec. 1953, Part III, June 1958.

[10] Rabeneck, G. L., Shumpert, P. K. and Sutton, J. F., "Steady Flow Ejector Research Program," Final Rept. for Contract Nonr-3067(00), AD 251 179, Dec. 1960.

[11] Armstrong, R. S., "Experimental Analysis for Low Area Ratio and Short Length Ejectors," Document No. D6-7928, Boeing Airplane Company (Transport Division), Dec. 1961.

[12] Reid, J., "The Effect of a Cylindrical Shroud on the Performance of a Stationary Convergent Nozzle," A.R.C., London, R&M 3320, Jan. 1962.

[13] Quinn, B. and Toms, H. L., "Calibration of a High Temperature and Pressure Ejector Facility with Back Pressure Effects," Aerospace Research Laboratories Rept., ARL-TR-0226, June 1975.

[14] Quinn, B. and Toms, H. L., "Mixing Duct Pressure Distributions and Exhaust Flow Characteristics of a High Temperature and Pressure Cylindrical Ejector," Aerospace Research Laboratories Rept., ARL-TR-75-0227, June 1975.

[15] Rosfjord, T. J. and Toms, H. L., "Recent Observations Including Temperature Dependence on Axisymmetric Jet Screech," *AIAA Journal*, Vol. 13, Oct. 1975, pp. 1384-1386.

[16] Quinn, B., "Effect of Aeroacoustic Interactions on Ejector Performance," *Journal of Aircraft*, Vol. 12, Nov. 1975, pp. 914-916.